

Effects of molecular adsorption on optical losses of the Ag (111) surface

A. V. Gavrilenko,* C. S. McKinney, and V. I. Gavrilenko

Center for Materials Research, Norfolk State University, 700 Park Avenue, Norfolk, Virginia 23504, USA

(Received 31 December 2009; revised manuscript received 19 June 2010; published 15 October 2010)

The first-principles density-functional theory is applied to study effects of molecular adsorption on optical losses of silver (111) surface. The ground states of the systems including water, methanol, and ethanol molecules adsorbed on Ag (111) surface were obtained by the total-energy minimization method within the local-density approximation. Optical functions were calculated within the random-phase approximation approach. Contribution of the surface states to optical losses was studied by calculations of the dielectric function of bare Ag (111) surface. Substantial modifications of the real and imaginary parts of the dielectric functions spectra in the near infrared and visible spectral regions, caused by surface states and molecular adsorption, were obtained. The results are discussed in comparison with available experimental data.

DOI: [10.1103/PhysRevB.82.155426](https://doi.org/10.1103/PhysRevB.82.155426)

PACS number(s): 31.10.+z, 68.43.-h

I. INTRODUCTION

The effects of metallic surface states and molecular adsorption on the atomic surface structure and electronic properties of transition metals are extensively discussed in literature (see, e.g., Refs. 1–4, and references therein). The silver based metallic nanostructures are actively studied for numerous applications of modern nanotechnology such as nanophotonics and nanoplasmonics.⁵ It has been demonstrated before that electronic surface states on metallic surfaces substantially contribute to the bonding of physisorbed atoms and molecules⁴ and to their optical absorption spectra.^{5,6} The semiclassical approach developed by Persson⁶ using Drude model and modified by Pinchuk *et al.*⁵ clearly demonstrated increasingly important contributions of the surface states on optical absorption spectra of metallic nanoparticles with decrease in their size.

Reduction of optical losses in nanostructured materials is one of the most important issues affecting successful engineering of different optoelectronics photonics devices. Optical losses of materials are determined through the imaginary part of the dielectric function $[\text{Im}(\epsilon)]$.⁷ Rather than compensating for the losses through external gain, electronic structure engineering of metallic nanoparticles by chemical adsorption could provide a more systematic way to reduce optical losses through redistribution of oscillator strength. However, this approach requires detailed understanding of electronic processes accompanied by chemical adsorption on a microscopic scale.

Recently using the first-principles modeling we predicted the effect of the surface states on the dielectric function spectra $[\epsilon(\omega)]$ of the nanometer-thick silver films.⁸ We showed that a decrease in the silver-slab thicknesses resulted in substantial increase in the $\text{Im}(\epsilon)$ due to the surface state contributions. Independently, these predictions have been confirmed experimentally by Drachev *et al.*⁹ by measuring reflectance and transmittance of differently shaped silver nanostructures simultaneously. They showed that the dramatic increase in $\text{Im}[\epsilon(\omega)]$ for both TE and TM light polarizations is due to the decrease in characteristic dimensions of the silver-based nanostructures, which agreed well with our predictions.⁸

In the present work, we study physical and chemical processes affecting optical losses of silver (111) surface that substantially contribute to the optics of metamaterials (the artificially fabricated nanomaterials⁹). The adsorption of water, ethanol, and methanol on silver nanofilms is studied by first-principles density-functional theory (DFT). Contribution of the surface states to optical losses is studied by calculations of the imaginary part of the dielectric function for metallic slabs of different thickness. We obtained substantial modifications of the optical function of metallic nanoslabs in the near infrared and visible spectral regions that are discussed in comparison with literature.

II. METHOD

Typical metallic nanoparticles are much bigger in size than the molecules studied. Consequently the interactions of small molecules with the nanoparticles can be studied using the widely used model of the surface physics: molecule on an atomic slab.¹⁰ Equilibrium atomic structures of silver surfaces with organic molecules are obtained from the total-energy minimization method within DFT using *ab initio* functionals.^{11,12} The basis functions are given numerically as values on an atomic-centered spherical-polar mesh, rather than as analytical functions (i.e., Gaussian orbitals), as implemented in the DMOL3 package.¹³ We employ the supercell approach to model the surface; our unit cell is a slab consisting of seven monolayers (MLs) of Ag(111)- $\sqrt{3} \times \sqrt{3}$, of which the top three layers were allowed to relax.

Explicit tests were performed to verify that the results were converged for the parameters given above with meshes up to $30 \times 30 \times 30$ for bulk and $16 \times 16 \times 1$ for surfaces. We note that optical data are converged to within 5% with the following meshes: $17 \times 17 \times 17$ for bulk and $6 \times 6 \times 1$ for surfaces. Increase in the Brillouin-zone sampling from the chosen mesh to the largest one tested improves results by only a few percent, which could be important for quantitative analysis; in this work, however, we opt for the smaller mesh since only relative changes are discussed. The DMOL3 (using localized basis) and CASTEP (using delocalized basis) packages deliver very close results for equilibrium geometry, however the DMOL3 yields data much faster than the CASTEP.

Consequently geometry optimization and calculations of adsorption energies have been performed by the DMOL3 package.

Previously, we carefully compared equilibrium geometries predicted by CASTEP and DMOL3 with different molecules^{14,15} and showed that the use of localized basis in DMOL3 is beneficial in terms of prediction of stable geometries. The geometries predicted by the DMOL3 local-density approximation (LDA) method are comparable to those predicted by the Vienna *ab initio* simulation package (VASP) (Ref. 16) when van der Waals contributions are taken into account during generalized gradient approximation (GGA) geometry optimizations. van der Waals contributions were approximated using the London dispersion formula^{17,18} as described in Ref. 19.

The stability of various equilibrium configurations is judged by the adsorption energy. The adsorption energy per molecule is defined as the difference between the total energy of the adsorption system and the energies of the isolated components, namely, the clean substrate and the adsorbate, divided by the number of adsorbed molecules N per unit cell,

$$E_{ads} = \frac{E_{tot} - (E_{substrate} + N \cdot E_{adsorbate})}{N}. \quad (1)$$

The electronic structure and optical properties of the system were calculated using *ab initio* norm-conserving (NC) pseudopotentials (PPs), as implemented in the CASTEP package.¹³ The eigenvalue problem was solved using the first-principles PP method with NC-PP.²⁰ Convergence of the results has been carefully checked by choosing energy cut-off values up to 1000 eV. The cut-off energy of 550 eV was chosen for NC-PP to ensure reliable convergence of predicted optical data. Choice of pseudopotentials (ultrasoft or norm-conserving) does not significantly affect the results. Exchange and correlation interaction is modeled using the Perdew-Burke-Ernzerhof formalism.²¹ Smearing of 0.2 eV is applied to the orbital projected density of states (PDOS) spectra.

Calculated self-consistent eigenenergies and eigenfunctions are used as inputs for optical calculations. Within its penetration depth beneath the surface, the incident light field $[E(\omega)]$ at frequency ω induces a linear optical susceptibility function $\chi^{(1)}$,

$$P_i(\omega) = \chi_{ij}^{(1)} E_j(\omega). \quad (2)$$

The function $\chi^{(1)}$ is then used to determine the complex dielectric function ($\varepsilon = \varepsilon_1 + i\varepsilon_2$) through the linear optical susceptibility: $\varepsilon = 1 + 4\pi\chi^{(1)}$. The dielectric function is determined through the contributions of both interband and intraband transitions. From the first principles we calculated only the interband term. The intraband (Drude) term is calculated according to $1 - \omega_p^2 / \omega(\omega + i\Gamma)$, where experimental values⁹ of plasma frequency ($\omega_p = 9.1$ eV) and corresponding broadening parameter ($\Gamma = 0.021$ eV) were taken to match measured data in infrared region.

Within the random-phase approximation (RPA) the interband function ε is given by²²

$$\varepsilon(\omega) = 1 - \frac{8\pi}{\Omega_0} \frac{1}{N} \sum_{\mathbf{k}} \sum_{c,v} \frac{\mathbf{p}_{cv}(\mathbf{k}) \mathbf{p}_{cv}^*(\mathbf{k})}{[E_c(\mathbf{k}) - E_v(\mathbf{k})]^2} F_{cv}(\omega, \mathbf{k}), \quad (3)$$

where Ω_0 is the volume of the supercell and indices c and v run over conduction (empty) and valence (filled) electron states, respectively. The spectral function $F_{cv}(\omega, \mathbf{k})$ at the incident light frequency ω is given by²²

$$F_{cv}(\omega, \mathbf{k}) = \frac{1}{\omega + i\eta - E_c(\mathbf{k}) + E_v(\mathbf{k})} + \frac{1}{-\omega - i\eta - E_c(\mathbf{k}) + E_v(\mathbf{k})}. \quad (4)$$

The ε represents the *local* part of the dielectric function. In this study we did not include nonlocalities due to the local field effect. Note that Eqs. (3) and (4) represent an effective value for the dielectric function averaged over different tensor component of $\varepsilon_{\alpha,\beta}$ (where $\alpha, \beta = x, y, z$) in direct space. A more detailed explanation can be found in Ref. 22.

III. RESULTS AND DISCUSSION

Realistic modeling of optical functions of solid surfaces and interfaces still remains challenging for first-principles theories.²³ As a first step it requires reliable reproduction of the ground state of the material (equilibrium atomic geometry) by minimizing the free energy; the optical properties could then be calculated using the optimized geometry as an input. Description of excited states, which could be in good agreement with experiment, normally requires inclusion of local field, many-body (excitons) effects, and probably other nonlocal contributions.^{24,25} This makes theory much more complicated than frequently used independent particles approach (or RPA).

In this work we focus on relative changes in electron-energy structure and optical response caused by molecular adsorption on Ag (111) surface, which could be realistically described without inclusion of many-body effects in optics.^{14,24} We study the nanostructures that incorporate quantum confinement effect, where the optical functions are thickness dependent in agreement with our previous finding by Zhu *et al.*⁸ that was confirmed experimentally by Drachev *et al.*⁹

A. Equilibrium geometries

Table I lists the adsorption energies E_{ads} , per molecule, as calculated by Eq. (1) and the optimized structural parameters of the adsorbates on the surface. Atomic relaxation of water on transition metals has been studied both theoretically and experimentally.^{1-3,26,27} The average surface height is used for the O-Ag and H-Ag distances, representing the distance between the surface and the oxygen/hydrogen. Since there are two H₂O molecules per unit cell, two distances are provided. Two different atomic geometries of water molecules physisorbed on Ag (111) surface are predicted: one of the two water molecules in the unit cell has a hydrogen pointing either up or down. Our predicted geometries of physisorbed water molecules on Ag (111) surface agree, for the most part,

TABLE I. Chemisorption and physisorption adsorption energies [as calculated by Eq. (1)] and optimized structural parameters of H_2O , CH_3OH , and $\text{CH}_3\text{CH}_2\text{OH}$ adsorbed on the Ag (111) surface. ΔAg is the difference in the average height of the top silver layer compared to a bare surface. O-H, O-O, and O-C represent the interatomic distances in the system; multiple distances are provided as needed.

Structure	E_{ads} (eV)	O-Ag (Å)	H-Ag (Å)	ΔAg (Å)	O-H (Å)	O-O (Å)	O-C (Å)
H_2O up	-0.9047	2.69, 2.95		+0.0007	0.978, 0.996, 1.01	2.78, 2.95, 2.98	
H_2O down	-0.9471	2.64, 3.18	2.06	+0.0155	0.994, 0.998, 1.01	2.84, 2.92, 2.94	
H_2O -down dsc	-0.1876	1.83, 2.25	0.846	+0.0233	0.986, 0.991, 1.06	2.51, 2.94, 3.37	
CH_3OH	-0.6017	2.51	2.24	+0.0017	0.985	5.00	1.42
CH_3OH dsc	+0.0622	1.46	0.968	+0.0375	2.94	5.00	1.39
$\text{CH}_3\text{CH}_2\text{OH}$	-0.6694	2.61	2.34	-0.0026	0.984	5.00	1.42
$\text{CH}_3\text{CH}_2\text{OH}$ dsc	+0.0004	1.48	0.911	+0.0272	2.96	5.00	1.40

well with those reported previously^{3,26,28} where a similar theoretical framework was used. The H_2O -up and H_2O -down geometries are shown in Figs. 1(a) and 1(b), respectively.

We also studied the effect of water molecule dissociation on optical properties of silver. At room temperature the reaction $\text{H}_2\text{O} \rightleftharpoons \text{HO}^- + \text{H}^+$ occurs spontaneously, the proton is then free to enter into reaction with the surface. Geometry optimization study indicates that the dissociated (dsc) H atom tends to interact much stronger with the surface. The same effect for water adsorbed on Ag (111), was reported earlier in Refs. 3 and 26. According to our total-energy minimization study, the dissociated hydrogen atom moved to the interstitial region. The adsorbed water pattern remarkably shifts while retaining the icelike hexagonal structure. For a single water molecule adsorbed on a closed-packed Ag (111) surface the distance between the oxygen and the host Ag atoms, the O-Ag distance, of 2.78 Å was reported in Ref. 26. In order to have water form icelike structures a surface

coverage of 0.66 ML was used. At higher surface coverages water begins to form additional icelike layers. Previously it was reported²⁸ that coverages less than 0.66 ML lead to remarkable modifications of the equilibrium geometries, in particular, near cluster boundaries. These modifications are expected to change optical spectra, however, the dynamics of surface coverage are out of scope of this study and will not be discussed any further.

For a single layer of H_2O adsorbed on the surface, the zigzag configuration of ice is not as pronounced as for water molecules not in contact with the surface. Our oxygen-silver surface distances can be found in Table I. The water hexagons are slightly irregular as can be seen in Figs. 1(a) and 1(b) and Table I (note the different O-O distances). The shift is much more pronounced in the H_2O -up configuration. This asymmetry of the hexagonal structure of water molecules was previously reported for $\text{Ru}\{0001\}$.²⁶ Once one of the hydrogen is desorbed, see Fig. 1(c), the remaining OH fragment shifts much closer to the surface resulting in symmetry reduction in the icelike hexagonal structure.

Though the average surface height does not change very much, see ΔAg in Table I, the individual silver atoms on the surface do move quite a bit more. This can be seen clearly in the side view of Fig. 1(b). Another observation is that the water molecules that do not lose their hydrogen are not oriented parallel to the surface, they are tilted with an angle of 7.69° . We report a negative adsorption energy of -0.1876 eV, as predicted by DMOL3, indicating the stable structure. This is contrary to what was reported in Refs. 26 and 27.

Methanol [CH_3OH , Fig. 1(d)] and ethanol [$\text{CH}_3\text{CH}_2\text{OH}$, Fig. 1(f)] adsorb very similarly on the surface of silver (see Table I), initially adsorbing with the hydroxide group. Once the O-H bond is broken, both molecules rotate bringing the oxygen atom closer to the surface and position themselves in configurations when the oxygen is centered above three Ag surface atoms [see Figs. 1(e) and 1(g)]. It is important to note that although a stable configuration was found with the O-H bond broken for both methanol and ethanol, those configurations are metastable at best, having positive adsorption energies of $+0.0622$ and $+0.0004$ eV. One can expect, however, that the van der Waals force correction may remarkably modify the adsorption energies¹⁹ thus yielding stable con-

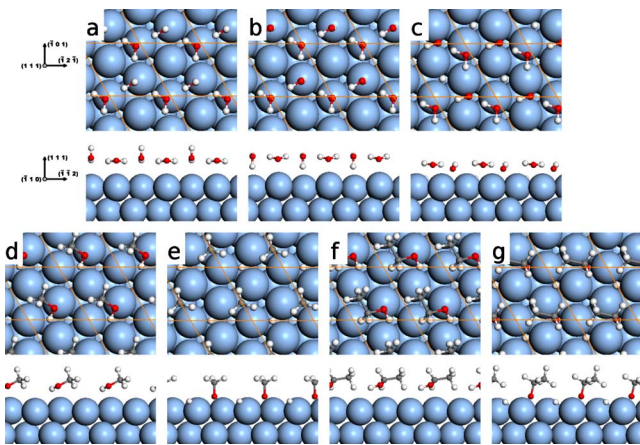


FIG. 1. (Color online) Top and side views of the optimized cell configurations of [(a)-(c)] water, [(d) and (e)] methanol, and [(f) and (g)] ethanol molecules adsorbed on Ag(111) surface. Panels represent the following configurations: (a) H_2O -up, (b) H_2O -down, (c) H_2O -down-dsc, (d) CH_3OH , (e) CH_3OH dsc, (f) $\text{CH}_3\text{CH}_2\text{OH}$, and (g) $\text{CH}_3\text{CH}_2\text{OH}$ dsc. The dsc configurations all have one hydrogen atom desorbed from the respective molecule and enter into a reaction with the surface.

figurations for dissociated geometries of both methanol and ethanol. Quantitative verification of this point is subject of a separate study.

B. Dielectric function and optical losses

Optical losses of a system are proportional to the imaginary part of dielectric susceptibility function, $[\text{Im}(\epsilon)]$.^{7,10,29} Here we discuss the $\text{Im}(\epsilon)$ spectra calculated according to Eqs. (3) and (4) for a 7-ML-thick Ag (111) slab with and without adsorbed molecules.

Optical spectra of bulk Ag in visible and near ultraviolet region reported in Refs. 30 and 31 are nearly identical and for the sake of simplicity we chose to use only the data from Ref. 30 in our comparisons. The infrared part of the spectrum calculated with adjusted parameters for plasma frequency agrees well with the experimental data, as shown in Fig. 2. It should be noted that in order to achieve better agreement of calculated bulk Ag optical spectra with experiment, the GW correction is needed.³² In this work, however, we mostly focus on the effects of molecular adsorption avoiding very time-consuming GW calculations for the surface. Consequently, presented spectra in visible and ultraviolet regions are redshifted to the measured data.

First, the predicted optical spectra for bare Ag (111) surface are considered. Without quasiparticle correction the predicted $\text{Im}(\epsilon)$, calculated using LDA with the experimental lattice constant, shows a remarkable redshift in comparison with experiment. In this work we use the LDA optimized lattice constant, which produces a compressed lattice of bulk Ag, for subsequent calculations of optical properties using GGA. The effect of lattice compression on electron-energy structure results in blueshift of optical spectra³³ thus improving a comparison with experiment.

Optical excitations from the surface states are responsible for the calculated increase in $\text{Im}(\epsilon)$ of Ag slab in visible and near infrared optical range with respect to bulk [see $\text{Im}(\epsilon)$ data between 1 and 2.5 eV in Fig. 2]. In order to understand the nature of predicted changes in the spectra of $\text{Im}(\epsilon)$ the PDOS spectra are calculated for the systems studied. Details of the calculations of PDOS are described in Ref. 22. Our previous analysis of calculated band structure and PDOS of the Ag slab (without molecules) (Ref. 8) indicated substantial contributions of surface electron-energy states which are in resonance with the bulk electron states and caused redistribution of the resulting density of states. In this paper we present the PDOS spectra analysis and focus on the effects on PDOS caused by the molecular adsorption.

Optical transitions between the occupied states and Fermi surface are responsible for the predicted substantial increase in the $\text{Im}(\epsilon)$ spectra of Ag (111) surface as compared with bulk in the near infrared region as demonstrated in Fig. 2. The transitions between the occupied states near -1.6 eV and Fermi level are responsible for the calculated shoulder at 1.55 eV in $\text{Im}(\epsilon)$ spectra of bare surface, as shown in Fig. 2.

Crystal truncation results in a predicted redistribution of charge between $4d$ and $5s$ orbitals causing effective energy shift of the $4d$ orbitals toward lower energies (see Fig. 2). Based on the PDOS data analysis we can state that predicted

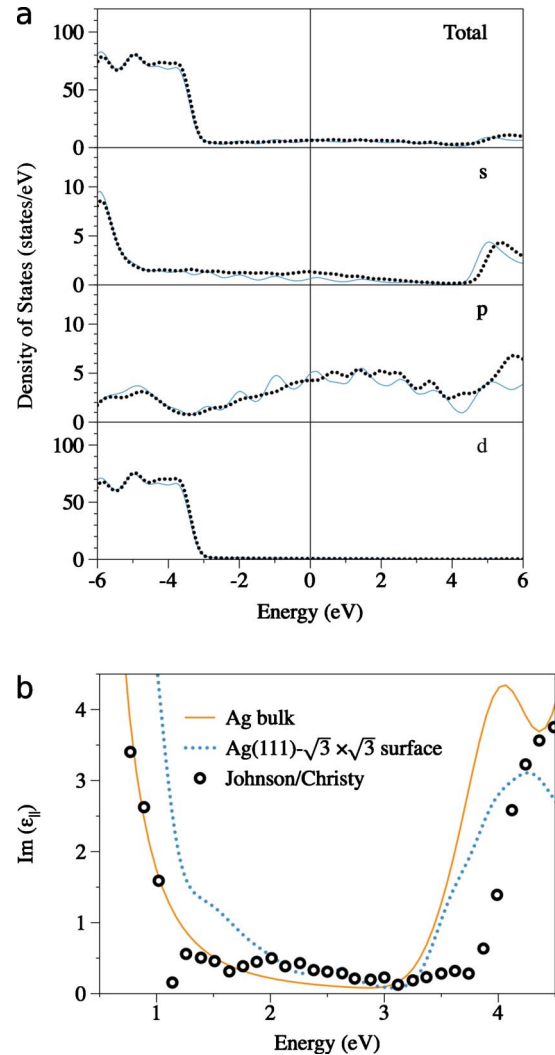


FIG. 2. (Color online) (a) Projected density of states of bulk (solid, blue) and 7-ML-thick slab (dotted, black) of silver. The shift of the d -orbitals is due to the redistribution of electrons between bulk and surface. (b) Calculated spectra of the imaginary part of dielectric susceptibility function for bulk (solid, orange) and 7-ML-thick Ag (111) slab (dotted, blue) in comparison with experimental data measured in Ref. 30 (circles).

modifications of the $\text{Im}(\epsilon)$ spectra of Ag (111) surface with respect to bulk are caused by surface-to-bulk and bulk-to-surface optical transitions. This conclusion is similar to previously reported analysis,³⁴ thus confirming bulk-to-surface nature of relevant electron transitions. Optical features predicted on Ag (111) above 3.5 eV are characterized by bulk electron transitions with minor contributions of the surfaces electrons.

In a separate paper⁸ we discussed the convergence of Ag dielectric function spectrum with slab thickness. It was shown that contribution of quantum confinement and surface states in 7 ML slab results in substantial changes in optical spectra, e.g., redshift up to 0.3 eV compared to bulk data in visible and near ultraviolet regions.⁸ Our predictions of additional molecular adsorption on a thin Ag slab will be useful for comparison with experimental data measured on nanostructured composite materials that incorporate both effects

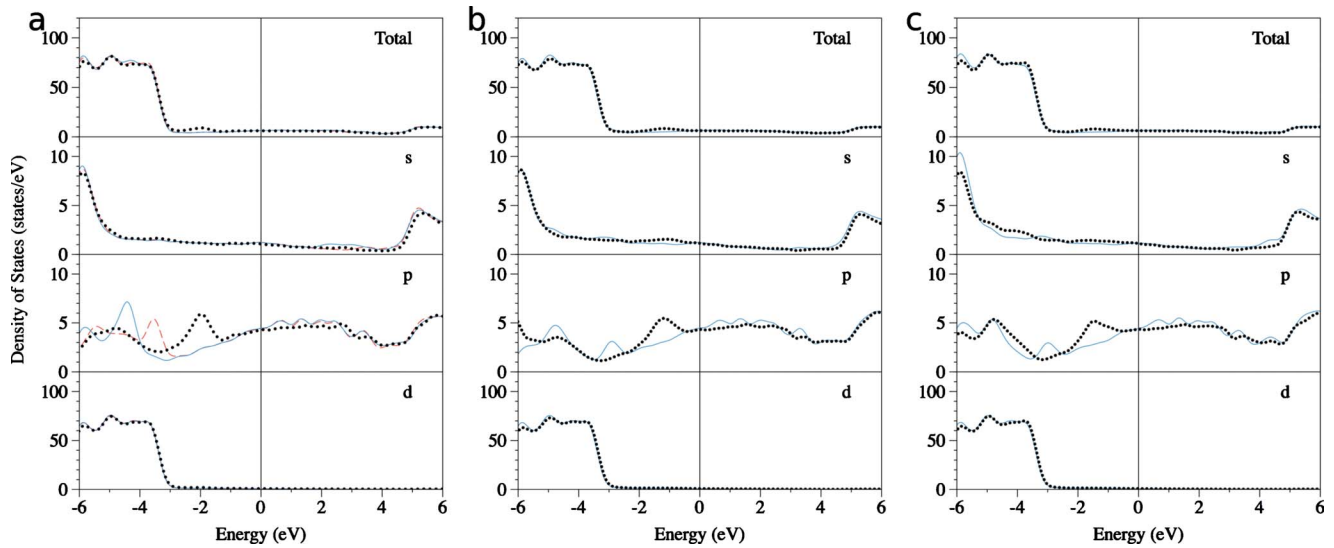


FIG. 3. (Color online) Projected density of states spectra of (a) H_2O , (b) CH_3OH , and (c) $\text{CH}_3\text{CH}_2\text{OH}$ adsorbed on Ag (111) film. The thin blue (solid) and red (dashed) lines depict the physisorbed configurations of (a) H_2O -up (blue, solid) and H_2O -down (red, dashed), (b) CH_3OH , and (c) $\text{CH}_3\text{CH}_2\text{OH}$; the dotted black line represents the chemisorbed configurations. The upper panel shows the total DOS and the other panel present orbital projected DOS as indicated by the panel indexes. The PDOS of bulk and silver surface can be found in Fig. 2 for comparison.

of molecular adsorption and quantum confinement, as recently reported in Ref. 9.

At room temperature most solutions contain dissociated molecules which could interact with the surface states.¹⁰ In Fig. 3 we present the effects of molecular adsorption on the calculated PDOS spectra of a Ag (111) film. On the bare Ag (111) surface the electron-energy structure is substantially modified as compared to the bulk Ag. Molecular adsorption on the crystal surface and atomic structure relaxation resulted in substantial overall increase in DOS related to the $5s$ and $4p$ orbitals as shows in Fig. 3. We observed at least two pronounced PDOS $5s$ peaks located near -0.4 and -1.6 eV (occupied states) on Ag (111) surface as well as energy increase in both $5s$ - and $4p$ -unoccupied states in the region between 0 and 4 eV. No substantial differences between the surface and bulk of the $4d$ -unoccupied PDOS has been observed.

Analysis of the PDOS spectra shows that changes in molecular orientations on Ag (111) surface result in modifications of mostly unoccupied p -electron states around 1.6 eV and higher. Effect of water molecule orientation on the surface (from “up” to “down” configuration) results in change in the $4p$ -related occupied orbital shift from -5.5 to -3.5 eV that corresponds to the minor observed modification of optical spectrum in the near UV region (see Fig. 4). Dissociation of hydrogen leads to further substantial increase in $\text{Im}(\epsilon)$ function and optical losses of Ag (111) in infrared and visible spectral regions.

Comparative analysis of the calculated PDOS spectra of Ag (111) surface with dissociated molecules and that of bulk Ag show strong modifications of the electron density: appearance of new occupied states located at around -1.7 to -2.5 eV below Fermi energy and unoccupied states near 0.5 – 0.7 eV above the Fermi level. Consequently, in dissociative configuration there are contributions to the $\text{Im}(\epsilon)$ func-

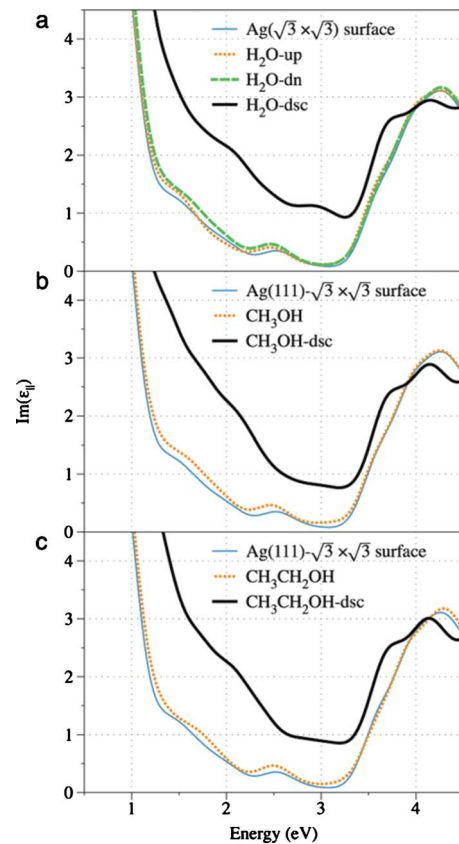


FIG. 4. (Color online) Imaginary part of calculated dielectric function of (a) water, (b) methanol, and (c) ethanol adsorbed on $\text{Ag}(111)-\sqrt{3}\times\sqrt{3}$ surface. The thin, dotted, and dashed lines represent the undissociated configuration while the bold solid lines correspond to dissociated molecules on the surface, respectively.

tion of electron transition—between occupied surface states and Fermi surface and between occupied and unoccupied surface states. The corresponding energy separations are between 1.5 and 3.2 eV. Contributions of the transitions between Fermi surface and unoccupied host states to the observed changes seem to be minor. Our results therefore indicate that chemical reactions between dissociated H and O atoms occur mostly with unpaired $5s$ - and $4p$ -surface electrons of the Ag atoms.

Obtained strong hybridizations of the host Ag $4d$ and Ag $2p$ electrons of oxygen is a result of molecular dissociation. The rehybridization of host electron orbitals results in observed increase in the oscillator strength in near infrared and visible regions. Our analysis of space charge distribution clearly indicate that most changes occur in the upper most monolayers of the slab thus indicating surface nature of this effect.

IV. CONCLUSIONS

Predicted strong increase in optical losses in infrared and visible range apparently dominates in the near UV region (see Fig. 4). According to the PDOS spectra the d electrons are involved in optical excitations in the region above 3.2 eV. In contrast to the infrared and visible region, the molecular adsorption in ultraviolet somewhat even reduces optical losses in the region above 4.0 eV (see Fig. 4) due to the discussed charge redistribution in the near-the-surface region. These findings should be interesting for the optical engineering of the UV devices.

Analysis of the data presented in Figs. 2 and 4 indicates several features related to the effect of molecular adsorption on the Ag (111) surface. Physisorption only slightly modifies the $\text{Im}(\epsilon)$ spectra mostly due to minor changes in atomic geometries. As expected, the most substantial observed modifications of the $\text{Im}(\epsilon)$ spectra are caused by chemisorption. Adsorption of molecules substantially enhances optical losses in infrared and visible regions. Comparison with PDOS spectra indicates redistribution of the charge associated with $5s$ and $4p$ silver orbitals (see Fig. 3). Another important feature in calculated optical spectra is the quantum confinement shift in the 7-ML-thick slab as compared to the bulk.

The results of this study clearly demonstrate strong contribution of the surface states to the optical losses on Ag (111) surface. Adsorption of organic molecules (water, methanol, and ethanol) results in further increase in the losses on Ag (111) surface. The observed increase in the $\text{Im}(\epsilon)$ function of Ag (111) surface, induced by molecular adsorption, is attributed to the substantial modifications of surface electron-energy structure and dramatic enhancement of electron transitions oscillator strengths between surface and bulk states.

ACKNOWLEDGMENTS

Authors acknowledge helpful discussions with M. A. Noginov, V. M. Shalaev, and V. P. Drachev. This work is supported by NSF PREM under Grant No. DRM-0611430, NSF NCN under Grant No. EEC-0228390, and by AFOSR under Grant No. FA9550-09-1-0456.

*a.v.gavrilenko@spartans.nsu.edu

- ¹M. Methfessel, D. Hennig, and M. Scheffler, *Phys. Rev. B* **46**, 4816 (1992).
- ²K. Morgenstern and J. Nieminen, *Phys. Rev. Lett.* **88**, 066102 (2002).
- ³A. Michaelides, *Appl. Phys. A* **85**, 415 (2006).
- ⁴F. Forster, A. Bendounan, J. Ziroff, and F. Reinert, *Phys. Rev. B* **78**, 161408 (2008).
- ⁵A. Pinchuk, U. Kreibitz, and A. Hilger, *Surf. Sci.* **557**, 269 (2004).
- ⁶B. N. J. Persson, *Surf. Sci.* **281**, 153 (1993).
- ⁷B. E. A. Saleh and M. C. Teich, *Fundamentals of Photonics*, 2nd ed. (Wiley, Hoboken, New Jersey, 2007).
- ⁸G. Zhu, M. Mayy, M. Bahoura, B. A. Ritzo, H. V. Gavrilenko, V. I. Gavrilenko, and M. A. Noginov, *Opt. Express* **16**, 15576 (2008).
- ⁹V. P. Drachev, U. K. Chettiar, A. V. Kildishev, H.-K. Yuan, W. Cai, and V. M. Shalaev, *Opt. Express* **16**, 1186 (2008).
- ¹⁰K. Kolasinski, *Surface Science. Foundation of Catalysis and Nanoscience*, 2nd ed. (Wiley, New York, 2008).
- ¹¹B. Delley, *J. Chem. Phys.* **92**, 508 (1990).
- ¹²B. Delley, *J. Chem. Phys.* **113**, 7756 (2000).
- ¹³Accelrys Inc, MATERIALS STUDIO, v 4.2, <http://www.accelrys.com/products/materials-studio/>, 2007.
- ¹⁴V. I. Gavrilenko, *Lecture Notes in Computer Science* (Springer-

Verlag, Berlin, 2006), p. 89.

- ¹⁵A. V. Gavrilenko, T. D. Matos, C. E. Bonner, S.-S. Sun, C. Zhang, and V. I. Gavrilenko, *J. Phys. Chem. C* **112**, 7908 (2008).
- ¹⁶G. Kresse and J. Furthmüller, *Comput. Mater. Sci.* **6**, 15 (1996).
- ¹⁷F. London, *Z. Phys.* **63**, 245 (1930).
- ¹⁸F. London, *Z. Phys. Chem.* **B11**, 222 (1930).
- ¹⁹F. Ortmann, W. G. Schmidt, and F. Bechstedt, *Phys. Rev. Lett.* **95**, 186101 (2005).
- ²⁰M. Fuchs and M. Scheffler, *Comput. Phys. Commun.* **119**, 67 (1999).
- ²¹J. P. Perdew, K. Burke, and M. Ernzerhof, *Phys. Rev. Lett.* **77**, 3865 (1996).
- ²²V. I. Gavrilenko, in *Tutorials in Complex Photonic Media*, edited by G. Dewar, M. W. McCall, M. A. Noginov, and N. Zheludev (SPIE Press, Bellingham 2009), Chap. 15, pp. 479–524.
- ²³M. C. Downer, B. S. Mendoza, and V. I. Gavrilenko, *Surf. Interface Anal.* **31**, 966 (2001).
- ²⁴V. I. Gavrilenko and F. Bechstedt, *Phys. Rev. B* **55**, 4343 (1997).
- ²⁵R. Leitsmann, W. G. Schmidt, P. H. Hahn, and F. Bechstedt, *Phys. Rev. B* **71**, 195209 (2005).
- ²⁶A. Michaelides, V. A. Ranea, P. L. de Andres, and D. A. King, *Phys. Rev. Lett.* **90**, 216102 (2003).
- ²⁷S. Meng, E. G. Wang, and S. Gao, *Phys. Rev. B* **69**, 195404 (2004).

- ²⁸A. Michaelides and K. Morgenstern, *Nature Mater.* **6**, 597 (2007).
- ²⁹J. E. Sipe and E. Ghahramani, *Phys. Rev. B* **48**, 11705 (1993).
- ³⁰P. B. Johnson and R. W. Christy, *Phys. Rev. B* **6**, 4370 (1972).
- ³¹K. Stahrenberg, T. Herrmann, K. Wilmers, N. Esser, W. Richter, and M. J. G. Lee, *Phys. Rev. B* **64**, 115111 (2001).
- ³²A. Marini, R. DelSole, and G. Onida, *Phys. Rev. B* **66**, 115101 (2002).
- ³³R. M. Martin, *Electronic Structure: Basic Theory and Practical Methods*, 2nd ed. (Cambridge University Press, New York, 2005).
- ³⁴P. Monachesi, M. Palumbo, R. Del Sole, R. Ahuja, and O. Eriksson, *Phys. Rev. B* **64**, 115421 (2001).